The DNA-Binding Domain of the Ultraspiracle Drives Deformation of the Response Element Whereas the DNA-Binding Domain of the Ecdysone Receptor Is Responsible for a Slight Additiona...

ARTICLE *in* BIOCHEMISTRY · FEBRUARY 2006

Impact Factor: 3.02 · DOI: 10.1021/bi051354b · Source: PubMed

Articles

The DNA-Binding Domain of the Ultraspiracle Drives Deformation of the Response Element Whereas the DNA-Binding Domain of the Ecdysone Receptor Is Responsible for a Slight Additional Change of the Preformed Structure†

Piotr Dobryszycki,‡ Iwona Grad,‡,§ Tomasz Krusiński, Piotr Michaluk,|| Dorota Sawicka, Agnieszka Kowalska, Marek Orłowski, Michał Jakób, Grzegorz Rymarczyk, Marian Kochman, and Andrzej Ożyhar*

Division of Biochemistry, Institute of Organic Chemistry, Biochemistry and Biotechnology, Wrocław University of Technology, Wybrzeże Wyspiańskiego 27, 50-370 Wrocław, Poland

Received July 13, 2005; Revised Manuscript Received October 28, 2005

ABSTRACT: Ecdysteroids control molting and metamorphosis in insects via a heterodimeric complex of two nuclear receptors, the ecdysone receptor (EcR) and ultraspiracle protein (Usp). We used fluorescence resonance energy transfer (FRET) to study the topology of the natural pseudopalindromic element from the *hsp27* gene (*hsp27pal*) in complex with the DNA-binding domains of Usp and EcR (UspDBD and EcRDBD, respectively). Steady-state data revealed shortening of the end-to-end distance of the *hsp27pal*-derived probe. For the 70.8 ± 0.6 Å distance obtained for the UspDBD-complexed DNA a bend of about 23.1 ± 2.9° was measured. Nearly the same value (23.0 ± 3.4°) was obtained for the DNA complexed with the UspDBD/EcRDBD heterodimer. The respective bend angles estimated using fluorescence decay measurements were 19.0 ± 2.1° and 20.9 ± 3.6°. Thus, the FRET data suggest for the first time that the UspDBD defines the architecture of the UspDBD/EcRDBD heterocomplex due to the significant deformation of the *hsp27pal*. This suggestion has been further reinforced using gel retardation experiments, which, in conjunction with high-resolution DNase I footprinting, indicate that the main contribution to the observed bend is given by the UspDBD itself, while binding of the EcRDBD molecule brings on a slight additional change of the preformed structure.

Nuclear receptors constitute a large group of transcription factors that are involved in many important biological processes. The receptors exert their action via binding to specific DNA sequences called response elements either as monomers or as dimers (*1*). For some members of this largest superfamily of metazoan transcription factors it has been shown that they induce a substantial distortion in the DNA structure, which may influence the transcription-inducing activity of the complex (*2*−*6*). Ecdysteroids are hormones that function as the major inducing signals responsible for regulation of postembryonic development in insects and possibly in other arthropods (*7*). The functional receptor for ecdysteroids is a transcription factor comprised of two nuclear receptors, the ecdysone receptor (EcR,[1] NR1H1) and a homologue of the mammalian retinoid X receptor, the ultraspiracle protein (Usp, NR2B4) (*8*, *9*). The Usp/EcR heterodimer binds ecdysone response elements after binding to the steroid hormone 20-hydroxyecdysone (20E) and consequently stimulates transcription of targeted genes (*10*). It has also been shown that the Usp/EcR heterodimer inhibits transcription in its unliganded state (*11*). Although molecular studies of the Usp/EcR heterodimer are much less extensive than those of vertebrate heterodimeric receptors, it is already clear that the ecdysteroid receptor complex, which exhibits mixed-type characteristics typical for both steroid and nonsteroid receptors, holds an exceptional position among the nuclear receptor family. One of its most intriguing features is propensity for response elements arranged as highly degenerated palindromes with a single intervening nucleotide [see Niedziela-Majka et al. (*12*) for a review]. This clearly distinguishes the Usp/EcR complex from vertebrate counterparts which tend to form complexes on inherently asymmetric DNA-binding sites composed of directly repeated half-sites (*13*). Our mutational studies on the interaction of the Usp and the EcR DBDs (UspDBD and EcRDBD, respectively) with the highly degenerated pseudopal-

† This research has been funded by a grant (3P04B 009 23) from the Polish State Committee for Scientific Research.

* Corresponding author. Phone: +48 (71) 3206333. Fax: +48 (71) 3206337. E-mail: andrzej.ozyhar@pwr.wroc.pl.

‡ The authors wish it to be known that, in their opinion, the first two authors should be regarded as joint first authors.

§ Present address: Département de Biologie Cellulaire, Université de Genève, 30, Quai Ernest-Ansermet, CH-1211 Genève 4, Switzerland.

|| Present address: The Nencki Institute of Experimental Biology, Pasteura 3, 02-093 Warsaw, Poland.

[1] Abbreviations: Cy-5, carboxymethylindocyanine *N*-hydroxysuccinimidyl ester; DBD, DNA-binding domain; EcR, ecdysone receptor; EcRDBD, EcR DNA-binding domain; 20E, 20-hydroxyecdysone; FRET, fluorescence resonance energy transfer; FL, fluorescein; *hsp27*, DNA sequence encoding hsp27 protein; *hsp27pal*, natural 20-hydroxyecdysone response element consisting of an imperfect palindrome from the promoter region of the *Drosophila hsp27* gene; IR-1, idealized element organized as an inverted repeat separated by 1 bp; TMRh, tetramethylrhodamine; Usp, ultraspiracle protein; UspDBD, Usp DNA-binding domain.

10.1021/bi051354b CCC: $33.50
Published on Web 12/22/2005

indromic response element from the *hsp27* gene promoter (*hsp27pal*) (*14*, *15*) have demonstrated that natural pseudopal-indromic ecdysone response elements may act as functionally asymmetric elements that locate the Usp/EcR heterodimer in a specific orientation (*12*). In particular, it has been shown that the UspDBD, which preferentially binds the 5′ half-site of the *hsp27pal*, operates as a key factor ("an anchor") dictating the polarity of the heterocomplex (5′-UspDBD-EcRDBD-3′).

The results presented in this work show for the first time that the natural element bound by the UspDBD/EcRDBD heterocomplex is deformed. The use of two independent methods, fluorescence resonance energy transfer (FRET) and gel retardation analysis, allowed us to demonstrate that the interaction of the UspDBD with the *hsp27pal* sequence induces bending in this element. Interestingly, subsequent binding of the EcRDBD molecule, i.e., formation of the UspDBD/EcRDBD−*hsp27pal* complex, does not significantly change the overall distortion of the *hsp27pal*, though it is accompanied by a change in the pattern of the DNase I hypersensitive sites. Thus, we believe that the UspDBD seems to be a molecule, which defines the architecture of the heterocomplex, not only due to the preferential binding of the 5′ half-site but also due to the significant deformation of the *hsp27pal*. Simultaneously, the EcRDBD induces only a slight additional change in the preformed structure.

MATERIALS AND METHODS

Preparation of the Fluorescently Labeled DNA. The following oligonucleotides, containing fragments of the *hsp27* gene promoter, including the *hsp27pal* sequence (*14*) (underlined), were used in the FRET experiments: **FL**-5′-CAA GGG TTC AAT GCA CTT GTC-3′ (O1), **TMRh**-5′-GAC AAG TGC ATT GAA CCC TTG-3′ (O2), and 5′-GAC AAG TGC ATT GAA CCC TTG-3′ (O3). The oligonucleotides were obtained from Eurogenetec S.A. (Belgium) (O1) and Biomers (Germany) (O2 and O3). The dyes fluorescein (FL) and tetramethylrhodamine (TMRh) are coupled to the 5′ ends of the respective oligonucleotide strands via a C_6 linker. The double-stranded DNA was annealed by hybridizing equal amounts of labeled, single-stranded oligonucleotides in 50 mM Tris-HCl, 100 mM NaCl, 10% (v/v) glycerol, and 5 μM $ZnCl_2$ (pH 7.8) with slow cooling from 95 to 20 °C overnight. The sequence of the final 21 bp long DNA molecule (*hsp27pal/FRET*) containing the *hsp27pal* sequence (underlined) used in the FRET experiments is

FL – 5′ – CAA GGG TTC AAT GCA CTT GTC – 3′ (O1)

3′ – GTT CCC AAG TTA CGT GAA CAG – 5′ - **TMRh** (O2)

For some control experiments (see Results) the ds oligonucleotide was prepared using unlabeled ss oligonucleotide O3 instead of O2. The labeling efficiencies were checked spectrophotometrically using the following absorption coefficients: $\epsilon_{260} = 221700\ M^{-1}\ cm^{-1}$ (O1), $\epsilon_{260} = 228500\ M^{-1}\ cm^{-1}$ (O2 and O3) (all estimated from a weighted average of the monomer nucleotide extinction coefficients: 15400 $M^{-1}\ cm^{-1}$ for A, 7400 $M^{-1}\ cm^{-1}$ for C, 11500 $M^{-1}\ cm^{-1}$ for G, and 8700 $M^{-1}\ cm^{-1}$ for T as described on the Genosys website http://www.genosys.com), $\epsilon_{494} = 65000\ M^{-1}\ cm^{-1}$ for fluorescein (*16*), and $\epsilon_{560} = 91000\ M^{-1}\ cm^{-1}$ for tetramethylrhodamine (*17*). The labeling stoichiometry was found to be ca. 1.0 for all of the labeled ss DNAs. Absorption spectra were measured with a Cary 3E UV−Vis spectrophotometer (Varian Inc., Scientific Instruments, Mulgrave, Australia).

Protein Preparation. The expression and purification of the UspDBD and the EcRDBD proteins were performed essentially as previously described for the mutant UspDBDs (*18*). To improve the purity of the final DBDs, one additional step was added to the procedure. In particular, DBD-containing fractions from the glutathione−Sepharose 4B column were applied on a 1 mL heparin−Sepharose CL-6B column equilibrated with 20 mM Tris-HCl, 150 mM NaCl, 1 mM DTT, and 5 μM $ZnCl_2$, pH 7.8 at 22 °C. Fractions of 1.0 mL were eluted at a flow rate of 0.25 mL/min with 10 mL of equilibration buffer and then with 10 mL of the same buffer containing 400 mM NaCl. DBD was eluted with 10 mL of equilibration buffer containing 650 mM NaCl, concentrated with an Amicon Ultra-4 centrifugal filter device (Millipore) to about 0.2 mL, and applied onto a Superdex 75 HR column operated as described previously (*19*). The DBDs were found to be at least 98% homogeneous when analyzed by SDS−PAGE (not shown). Concentrations of protein samples were determined using the following absorption coefficients: $\epsilon_{280} = 7000\ M^{-1}\ cm^{-1}$ (UspDBD); $\epsilon_{280} = 5840\ M^{-1}\ cm^{-1}$ (EcRDBD) (*19*).

Preparation of DNA Fragments for Gel Retardation Analysis. To construct the circular permutation vector containing the fragment of the *hsp27* gene promoter (*14*), including the *hsp27pal* sequence (pTZ-Bend-*hsp27*), the vector pBend2 (*20*) was digested using *Eco*RI and *Hin*dIII. The resulting 236 bp fragment, containing tandem restriction sites as well as unique cloning sites, was gel purified and ligated into pTZ57R plasmid (MBI Fermentas). The obtained construct was digested with *Sal*I, and the DNA fragment containing the *hsp27pal* (*14*) sequence was introduced by ligation with two synthetic oligonucleotides containing *Sal*I restriction sites (small letters): 5′-tcg aAG ACA AGG GTT CAA TGC ACT TGT CCA ATG-3′ and 5′-tcg aCA TTG GAC AAG TGC ATT GAA CCC TTG TCT-3′. The sequence of the resulting permutation fragment within the pTZ-Bend-*hsp27* vector was confirmed by sequencing. This vector was digested with either *Bam*HI, *Kpn*I, *Sma*I, *Eco*RV, *Xho*I, or *Nhe*I, producing 154 bp size fragments containing the *hsp27pal* sequence located in various positions corresponding to the 5′ end of the DNA fragment (see Figure 3A). The fragments were purified with a NAP-10 column (Amersham Biosciencs), dephosphorylated with shrimp alkaline phosphatase (Biotec Pharmacon), and labeled with [γ-^{32}P]ATP (Perkin-Elmer).

FRET: Steady-State and Lifetime Measurements. The efficiency of energy transfer, E_T, was determined based on steady-state and lifetime measurements. For each set of experiments, fluorescence spectra were obtained for the donor-labeled DNA, acceptor-labeled DNA, and doubly labeled samples. E_T from the fluorescence donor to an acceptor is related to the donor−acceptor distance (R) according to the equation (*21*):

$$E_T = 1 - F_{D-A}/F_D = 1 - \tau_{D-A}/\tau_D = R_0^6/(R_0^6 + R^6) \quad (1)$$

where F_{D-A}, F_D, τ_{D-A}, and τ_D are the fluorescence intensities

and lifetimes of a donor in the presence and absence of an acceptor, respectively. R_0 is the Förster distance at which the energy transfer efficiency, E_T, is 50% and is characteristic for a given donor−acceptor pair and can be calculated from

$$R_0 = (9.79 \times 10^3)(J\kappa^2 Q_D n^{-4})^{1/6}\ \text{Å} \quad (2)$$

The refractive index n was taken to be 1.4 (*22*), the orientation factor κ^2 was assumed to be $^2/_3$, which is a reasonable assumption taking into account the chemical nature of C_6 linkers and the data presented elsewhere based on limiting anisotropies (*23*−*26*), J is the spectral overlap integral, and Q_D is the donor quantum yield in the absence of an acceptor.

Steady-state fluorescence measurements were taken on a Fluorolog 3-21 (Jobin-Yvon, Spex, Horiba, Cedex, France) instrument. The samples were excited at 497 nm, and the emission spectra were recorded from 500 to 620 nm. Aliquots of 500 μL of DNA solutions were titrated with a 34 μM protein stock solution up to a final protein concentration of about 450 nM and incubated for 10 min for each titration step. All measurements were carried out at 25 °C.

Fluorescence lifetimes were determined with a multifrequency phase fluorometer, SLM 48000S (SLM Aminco, Urbana, IL). The excitation wavelength was 495 nm while emission was observed using a cutoff filter (Schott), OG 530. This filter allows observation of the donor fluorescence in the presence of an acceptor without any fluorescence contribution from the acceptor. Typically, the data points were collected in the range 1−140 MHz. The average donor lifetime was calculated from the equation $\langle\tau\rangle = \sum\alpha_i\tau_i$, where α_i represent the fractional amplitudes of the components and τ_i are the decay times (*27*). The data were analyzed using software supplied with the instrument.

The Geometric Model Used To Calculate the Bend Angle (ϕ) for the FRET Data. Calculation of the DNA bending angle (ϕ) was done as described by Lorenz et al. (*26*) and is based on the R and R_B values (see Figure 1B) obtained using FRET data for the doubly labeled straight sequence of B-DNA (free) and the doubly labeled kinked (protein-bound) sequence. Figure 1 displays the geometric model ["single central bend" (*28*)] used to evaluate a bend angle for the UspDBD and/or UspDBD/EcRDBD protein complex with the *hsp27pal*-containing ds oligonucleotide (*hsp27pal/FRET*). This model is based on the assumption that the bending arises along the helix axis and unwinding does not take place. The lengths of the vectors describing the positions of the dyes were determined and used to calculate the distance between the dyes. The hinge point of the bend was chosen as the midpoint of the 21 bp ds oligonucleotide (position 0 in Figure 1A). The zwitterionic TMRh has been assumed to stack on the top of the DNA helix whereas the FL is pointing away from the DNA at some angle (*26*) (Figure 1B). The α, γ, δ, and ϕ angles used in the model are defined in Figure 1B and described as follows:

$$c = (a^2 + b^2 - 2ab\cos\alpha)^{1/2} \quad (3)$$

$$\phi = 180° - (\gamma + \delta) \quad (4)$$

Gel Retardation Analysis. Electrophoretic mobility shift assays were performed under conditions previously described (*12*, *18*, *29*). Briefly, equal amounts (2 nM) of the respective permutation fragments were incubated with 50 nM UspDBD or with the equimolar mixture of the UspDBD and EcRDBD proteins. Binding was performed for 30 min on ice in the binding buffer: 10 mM Tris-HCl, pH 7.8, 150 mM NaCl, 5 μM $ZnCl_2$, 0.5 mg/mL ovoalbumin, 1 mM DTT, 10% (v/v) glycerol, and 400 ng of poly(dI-dC). Electrophoresis was performed in 5% polyacrylamide gel (acrylamide:bisacrylamide 75:1) in a 0.25 × TBE buffer at 4 °C. After 1.5 h at 160 V of prerun, gels were run at 270 V for 30 min and then at 200 V for 4 h. The migration distances of the DNA−protein complexes and free probes were determined with a Fuji Film FLA 3000 fluorescent image analyzer (Raytest Isotopenmessgeräte GmbH) and AIDA Bio-package software (Raytest Isotopenmessgeräte GmbH).

Calculation of the Bending Angle from Gel Retardation Experiments. The bending angle calculation was performed as described by Ferrari et al. (*30*). The magnitude of the distortion angle was determined graphically using SigmaPlot 8.0 software and the equation (*30*):

$$(\mu_b/\mu_f) = 2K(1 + \cos\theta)(D/L)^2 - 2K(1 + \cos\theta)(D/L) + K \quad (5)$$

where L is the length of the DNA fragment, and D is the distance from the protein-binding site to the 5′ end of the DNA fragment. K is a constant, θ is the internal DNA bending angle, μ_b is the electrophoretic mobility of the protein−DNA complex, and μ_f is the electrophoretic mobility of the free DNA. From a parabolic plot of the function $(\mu_b/\mu_f) = f(D/L)$ one can obtain the DNA bending angle (α) using the equation $\alpha = 180 - \arccos[(-b/2c) - 1]$, where b and c are the parabolic parameters of eq 5 (*30*) and the position of the hinge point by minimization of the function.

DNase I Footprinting Assay. The DNase I footprinting assay was performed according to Mischati et al. (*31*) with some modifications. Details will be published elsewhere. Briefly, DNase I footprinting patterns were generated in the presence of the UspDBD or the UspDBD/EcRDBD complex. The patterns, visualized with the ALF*express* DNA sequencer (Pharmacia Biotech), were obtained using reactions performed with 49 fmol of the Cy5-labeled 276 bp DNA fragment containing the *hsp27pal* sequence. The fragment was generated using PCR and recombinant pBluescript KS+/*hsp27* plasmid (*15*) as a template.

RESULTS

Detection of DNA Bending by Fluorescence Resonance Energy Transfer (FRET). Our previous study indicated differences in molecular mechanisms that underlie the *hsp27pal* recognition by the isolated UspDBD and its equimolar mixture with the EcRDBD. It has been demonstrated that the UspDBD binds as a monomer to the 5′ half-site of this sequence, whereas the UspDBD/EcRDBD heterodimeric complex is formed in a synergistic manner when both DBDs are incubated with *hsp27pal* (*12*). To find out whether the interaction of the UspDBD and/or the UspDBD/EcRDBD heterocomplex induces bending in the *hsp27pal* sequence, i.e., a change in the end-to-end distance, we decided to determine a distance-dependent energy transfer. We measured the FRET between two dye molecules, fluorescein (FL) and tetramethylrhodamine (TMRh), located

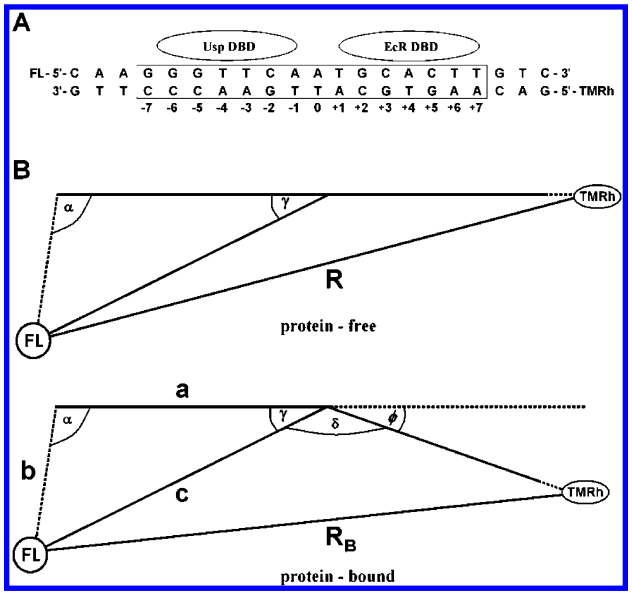

FIGURE 1: Geometry of the UspDBD/EcRDBD−DNA complex. (A) Sequence of the ds *hsp27pal/FRET* oligonucleotide used in the FRET studies. The sequence of the *hsp27pal* (*15*) is shown in frame [numbering according to Ożyhar and Pongs (*34*)]. (B) Schematic diagram of the model used to calculate the bend angle (ϕ) for the FRET efficiency data. The FL dye is allowed to bend away from the DNA axis at some angle (*26*), α. *R* and R_B denote the FRET distance between the fluorescence donor and acceptor in the protein-free (upper panel) and the protein-bound DNA (lower panel) (for details see the Materials and Methods section).

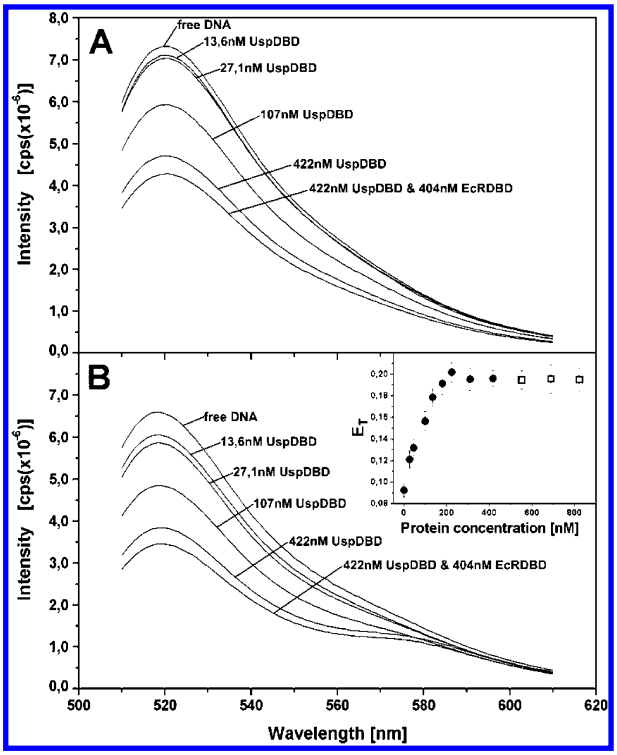

FIGURE 2: Examples of steady-state fluorescence emission spectra. (A) Control titration of singly labeled 25 nM *hsp27pal/FRET*. Protein concentrations are indicated above the appropriate curves. (B) Titration of doubly labeled *hsp27pal/FRET*. Inset: Equilibrium titration results of FRET efficiency change versus UspDBD concentration (closed circles). Titration of the *hsp27pal/FRET* in the presence of a constant UspDBD concentration (422 nM) with the EcRDBD in the range of 404−800 nM concentration (open squares). Energy transfer efficiency is determined from the decrease of FL donor emission. A correction was made for dilution and fluorescein photobleaching.

at the ends of the *hsp27pal/FRET* ds oligonucleotide (Figure 1) in complex with the UspDBD monomer or UspDBD/EcRDBD heterodimer. The efficiency of the energy transfer, E_T, was measured by monitoring the fluorescence emission intensity at 518 nm (λ_{ex} = 497 nm) where the FL label (donor) could be observed without interference from the TMRh (acceptor) emission. The spectra in Figure 2A represent a control experiment where the *hsp27pal/FRET* labeled only with FL was incubated either with the UspDBD only or with a mixture of the UspDBD and the EcRDBD. Figure 2B illustrates an analogous experiment carried out for the doubly labeled *hsp27pal/FRET*. In both experiments formation of the monomeric UspDBD−DNA complex results in a clear decrease in the fluorescence intensity. Addition of approximately equimolar amount of the EcRDBD, which promotes a synergistic formation of the heterodimeric UspDBD/EcRDBD complex (*12*), results in an additional decrease in the florescence intensity. The energy transfer from the FL probe to TMRh was observed only for doubly labeled DNA as an additional decrease in donor intensity observed at 520 nm and a respective increase of the 582 nm peak from acceptor emission (compare panels A and B of Figure 2). The E_T values for DNA titrated with the UspDBD and complexed with the UspDBD/EcRDBD heterodimer are shown in an inset to Figure 2B. The change of E_T from 0.092 ± 0.007 for free DNA to 0.196 ± 0.012 for the UspDBD−DNA complex resulted from the closer position of the donor−acceptor pair, i.e., from 79.1 ± 0.9 to 70.8 ± 0.6 Å (Table 1). Interestingly, formation of the UspDBD/EcRDBD heterodimer does not significantly change the E_T value (open squares in the inset to Figure 2B). The final value of E_T, 0.195 ± 0.015, for the UspDBD/EcRDBD−DNA complex resulted from a donor−acceptor end-to-end distance of 70.9 ± 0.7 Å (Table 1). For free DNA in solution the measured value of E_T, 0.092 ± 0.007, is consistent with the fact that the end-to-end distance for a 21 bp fragment of B-DNA should be about 72 Å. If one adds at least about 7 Å at each end to account for the distance added by flexible C_6 spacers with which the probes are attached to the DNA, then the expected distance would be around 86 Å. The experimental value (*R*) was 79.1 ± 0.9 Å, probably due to the attraction of the TMRh probe to the DNA helix, out of the DNA axis position of the FL probe and the flexibility of the spacers. Modeling the FL and TMRh dye positions at the DNA ends has shown that the FL probe is further away from the DNA, whereas the TMRh interacts with the DNA helix (*26*). Bending angles could be calculated based on the estimated distances between the DNA ends assuming that the bend is localized at the central A−T base pair (see Figure 1). Thus, for the 70.8 ± 0.6 Å distance obtained for the UspDBD-complexed DNA a bend of about 23.1 ± 2.9° was measured (Table 1). Nearly the same value was obtained for the DNA complexed with the UspDBD/EcRDBD heterodimer (Table 1). The fluorescence decay data confirm the results described above. They were obtained for the same protein and DNA preparations as steady-state measurements. Free FL in solution exhibits a single-exponential decay with a lifetime of 3.92 ns in 0.1 M NaOH [data not shown and Melcher et al. (*32*)]. However, when the probe is attached to the *hsp27pal/FRET* ds oligonucleotide, two exponentials are necessary to describe the decay curves (not shown). The averaged lifetime experiment data are presented in Table 1

Table 1: FRET Measurements of the End-to-End Distance and Bend Angles[a]

protein(s) in complex with *hsp27pal/FRET*	$\langle\tau_{DA}\rangle$ (ns)	$\langle\tau_D\rangle$ (ns)	E_T	R/R_B (Å)	ϕ (deg)
no			0.092 ± 0.007	79.1 ± 0.9	0
	(3.34)	(3.69)	(0.095 ± 0.006)	(78.8 ± 0.8)	(0)
UspDBD			0.196 ± 0.012	70.8 ± 0.6	23.1 ± 2.9
	(2.70)	(3.26)	(0.174 ± 0.007)	(72.1 ± 0.4)	(19.0 ± 2.1)
UspDBD/EcRDBD			0.195 ± 0.015	70.9 ± 0.7	23.0 ± 3.4
	(2.53)	(3.10)	(0.183 ± 0.014)	(71.5 ± 0.8)	(20.9 ± 3.6)

[a] Energy transfer efficiency (E_T) and end-to-end distance for protein-free (R) and for protein-bound (R_B) *hsp27pal/FRET* were obtained from steady-state and lifetime (in parentheses) measurements.

(in parentheses). For the UspDBD−DNA complex the 0.174 ± 0.007 value of E_T was determined. According to eq 1, this corresponds to a 72.1 ± 0.4 Å distance. For the heterodimeric complex the R_B value was 71.5 ± 0.8 Å (see Table 1). The respective bend angles are 19.0 ± 2.1° and 20.9 ± 3.6°. It has been previously shown that the UspDBD is a key factor which determines the anisotropy of the UspDBD/EcRDBD heterocomplex on the *hsp27pal* due to preferential binding to its 5′ half-site (*12*). Our data show, for the first time, that the UspDBD itself affects the architecture of the UspDBD/EcRDBD heterocomplex due to the significant deformation of the *hsp27pal*.

DNA Curvature Estimated by Gel Electrophoresis. Each method employed to measure the degree of DNA bending carries certain limitations. Therefore, we decided to determine the angle of the *hsp27pal* bend caused by UspDBD or the UspDBD/EcRDBD heterocomplex by combining gel retardation techniques, making use of the change of the electrophoretic mobility of a distorted DNA fragment. The mobility varies according to the site and degree of bending (*33*). A 29 bp fragment of the *hsp27* gene promoter containing the *hsp27pal* sequence was inserted at the *Sal*I site of a plasmid vector carrying two identical segments with many directly repeated restriction sites. The plasmid was then cleaved by the appropriate restriction enzymes, giving DNA fragments that were identical in size but differing in the location of the binding site (Figure 3A). Results presented in Figure 3B,C show that free (F), ^{32}P-labeled fragments migrate in polyacrylamide gel with similar mobility, which indicates the absence of the intrinsic *hsp27pal*-directed curvature. In contrast, fragments with a gradient of mobilities were generated by binding either the UspDBD monomer (inset in Figure 3B, complex CI_U) or the UspDBD/EcRDBD heterodimer (inset in Figure 3C, complex CII_{EU}). The differences in the mobilities of the particular restriction fragments are apparently very subtle, probably due to a small value of the bend angle. Nevertheless, multiple repetitions of the experiment and the range of a standard deviation suggest that the outcomes are credible. The data (Table 2) based on at least six independent experiments concur in a large measure with those obtained using FRET technology. Comparison of the apparent bending angles induced by the UspDBD (ca. 15.5°) and the UspDBD/EcRDBD heterocomplex (ca. 20.9°) again reinforces the suggestion that the main contribution to the observed bend is given by the UspDBD itself, while the binding of the EcRDBD brings on only a minor alteration of the preformed structure.

The fact that only the gel retardation method demonstrated a small though defined difference between the bend angles estimated for the UspDBD and the UspDBD/EcRDBD heterocomplex might be the result of different lengths of permutation fragments (154 bp) compared to the *hsp27pal/FRET* fragment (21 bp) used for the fluorescence experiments. Accordingly, some interactions important for bending might not have occurred for the 21 bp *hsp27pal/FRET* fragment. High-resolution DNase I footprinting experiments carried out with a 276 bp DNA fragment containing a part of the *hsp27* gene promoter, including the *hsp27pal*, suggest that the UspDBD and the EcRDBD cause some distortion in the ds DNA. Results presented in Figure 4A indicate that the formation of the UspDBD/EcRDBD−*hsp27pal* complex induces DNase I hypersensitive sites, commonly considered to be DNA structure change indicators, not only within the *hsp27* gene-derived fragment but also outside the sequence corresponding to the *hsp27pal/FRET* probe. Interestingly, in the case of the UspDBD the strongest hypersensitivity effect is observed for +6 residue (T) and a weaker effect is observed for T and C residues localized outside the *hsp*27*pal* sequence (Figure 4B).

DISCUSSION

The *hsp*27*pal* is the best described 20E-dependent natural regulatory element [see Niedziela-Majka et al. (*12*)]. It has been previously shown with the use of biochemical methods that it interacts with the 20E receptor (*15*), while a site-directed mutagenesis allowed the precise determination of the base pairs necessary for effective interaction (*18*, *29*, *34*). This regulatory element is also functional in vivo in tests with a reporter gene (*8*, *9*). Mutational analysis carried out in our laboratory with the recombinant DBDs of Usp and EcR proteins demonstrated that the *hsp*27*pal* acts as a functionally asymmetric element that locates the Usp/EcR heterodimer in a specific orientation. In particular, it has been shown that the UspDBD that preferentially binds the 5′ half-site of the *hsp27pal* is a key factor dictating the polarity of the heterocomplex (5′-UspDBD-EcRDBD-3′) (*12*). A similar architecture was observed in the crystallographic structure of the UspDBD/EcRDBD complex with the highly symmetrical IR-1 element (*35*) Interestingly, according to Devarakonda et al. (*35*), structure analysis indicated a lack of significant distortions of the IR-1 element except for the spacer. Since our present experiments clearly demonstrate that both the UspDBD alone and the UspDBD/EcRDBD heterocomplex induce the *hsp27pal* sequence to bend, we have reevaluated a coordinate file of the UspDBD/EcRDBD−IR-1 structure (PBD ID 1R0O) using the 3DNA structure analysis and rebuilding software package (*36*). The local helical parameters obtained from the 3DNA software were then used as an input into the Madbend program (*37*) for calculating the bend magnitude and global roll of DNA

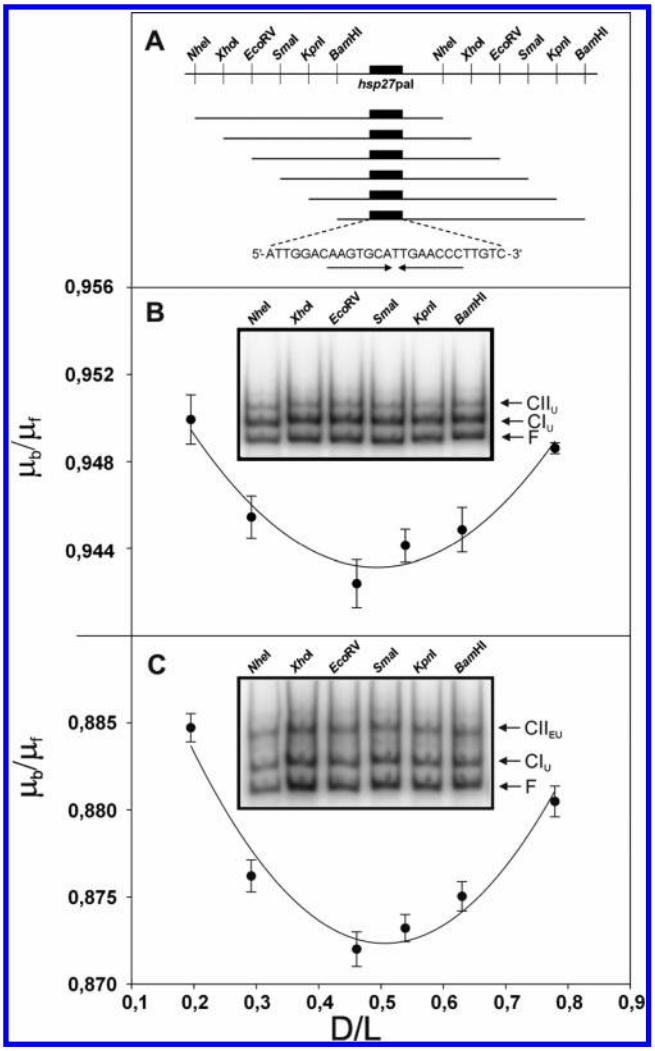

FIGURE 3: Gel retardation analysis of the UspDBD or the UspDBD/EcRDBD binding to the DNA fragments containing *hsp27pal*. (A) Schematic representation of 154 bp restriction fragments used for gel retardation experiments. A fragment of the *hsp27* gene promoter, including the *hsp27pal* sequence (*14*), was cloned into the plasmid pTZ57 containing an *Eco*RI−*Hin*dIII fragment from the pBend2 (*20*) vector. The resulting vector was digested with the indicated restriction enzymes producing 154 bp size fragments containing the *hsp27pal* sequence (note that for cloning purposes the sequence was inserted in reversed orientation) located in various positions corresponding to the 5′ end of the DNA fragment. For more details see the Materials and Methods section. (B) Function of the relative mobility (μ_b/μ_f) of the UspDBD-bound DNA and the relative distance of the protein-binding site (D/L). The graph represents the best fit of the cos function for six independent electrophoretic mobility shift gel experiments; representative gel analysis for the indicated restriction fragments is shown in the inset. Key: CI_U, a monomer of the UspDBD; F, free DNA; CII_U, a dimer of the UspDBD. (C) Analysis of the UspDBD-EcRDBD binding. (μ_b/μ_f) relative mobility of UspDBD-EcRDBD-bound DNA. Best fit of the cos function for seven independent experiments; representative gel analysis for the indicated fragments is shown in the inset. Key: CII_{EU}, a heterodimer of the UspDBD/EcRDBD; CI_U, a monomer of the UspDBD; F, free DNA. The identities of complexes in gel shift experiments were known from previous studies (*29*) and from equilibrium titration experiments (data not shown).

molecules. Calculations using Madbend with a reference plane in the middle of the IR-1 molecule resulted in the bend angle of 24.07° (Figure 5C). Thus, despite the observed bend angles being small, they can still be reliably observed with the use of independent techniques and different response elements. Recently, it was pointed out that the accumulation of information for various protein−DNA complexes is required for understanding the biological relevance of DNA bending through small angles (*38*).

Table 2: Bending Angles Obtained Using Gel Retardation Assay[a]

protein−DNA complex	bending angle (deg)
UspDBD−*hsp27pal*	15.5 (16.6−14.3)
UspDBD/EcRDBD−*hsp27pal*	20.9 (21.8−19.9)

[a] The lower and upper limits of the obtained data are presented in parentheses.

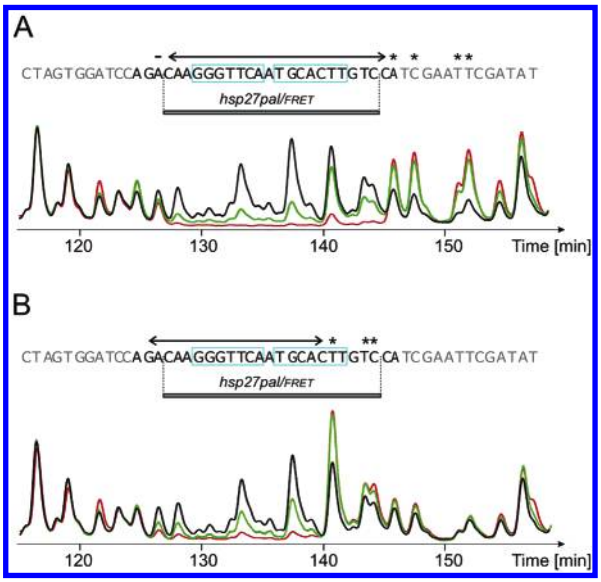

FIGURE 4: DNase I footprinting assay. The DNase I footprinting pattern generated by the UspDBD/EcRDBD heterodimer (A) or by the UspDBD (B). The protein concentrations were 0 nM (black line), 20 nM (green line), and 120 nM (red line). The patterns were obtained using reactions performed with 49 fmol of Cy5-labeled ds DNA fragment containing the *hsp27pal* and visualized with the ALF*express* DNA sequencer. The protected sequence is indicated by a bidirectional arrow above the *hsp27pal* (blue boxes) and the sequence corresponding to the *hsp27pal/FRET* probe by a gray line. Asterisks indicate hypersensitive sites, and the vector sequence is indicated in gray.

The DNA bend angles observed by fluorescence intensity measurements (ca. 23.1° for the UspDBD and 23.0° for the UspDBD/EcRDBD) are consistent with the values derived from the lifetime data (19.0°, 20.9°) and roughly with those obtained from gel mobility experiments (15.5°, 20.9°). As demonstrated above by high-resolution DNase I footprinting, the reason for a small, although detectable, difference between the bend angles estimated using gel retardation for the UspDBD and UspDBD/EcRDBD might be some subtle heterocomplex-induced changes of the DNA structure outside the sequence corresponding to the *hsp27pal/FRET* probe. Since the induction of the UspDBD/EcRDBD heterocomplex-specific hypersensitive sites is not accompanied by a significant alteration of the bending angle, we assume that the hypersensitive sites reflect local changes of the DNA structure important for the fine-tuning of protein−DNA interactions. It has been recently shown that, in contrast to the UspDBD, the EcRDBD appears to be an intrinsically unstructured protein-like (*39*−*41*) molecule with a high degree of intramolecular plasticity (*42*). Results presented here are consistent with this observation and point out the crucial role of the UspDBD in defining the overall architecture of the UspDBD/EcRDBD−*hsp27pal* complex, whereas

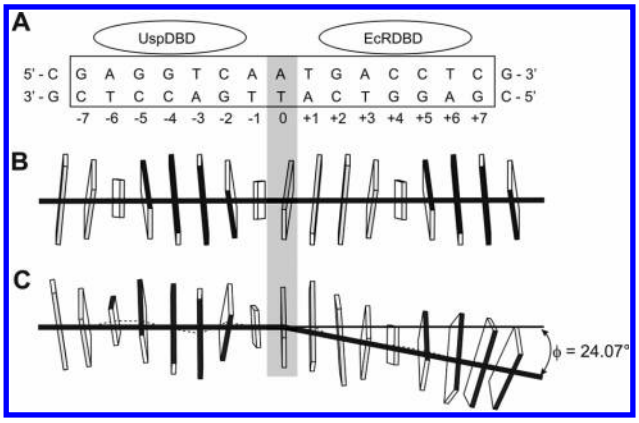

FIGURE 5: Reevaluation of the crystallographic data indicates bending of the IR-1 element. (A) Sequence of the ds oligonucleotide used in the crystallographic analysis (*35*) of the UspDBD/EcRDBD heterodimer complexed with the IR-1. The sequence of the idealized IR-1 element is shown in frame, and ovals represent localization of the respective DBDs. (B) A B-DNA-like model of the IR-1 ds oligonucleotide generated according to Vlahovicek et al. (*43*). (C) A model of the IR-1 ds oligonucleotide generated using the 3DNA software and a coordinate file of the UspDBD/EcRDBD−IR-1 structure (PDB ID 1R0O). DNA base pairs are shown as rectangular blocks, and the idealized helical axis based on the axis computed by the 3DNA software (*36*) (dotted line) is shown in black.

the pliable EcRDBD molecule is responsible for inducing local structure variations.

The *hsp27pal* bending forced by the UspDBD ("the anchoring factor"), in the context of the full-length proteins, might be an important step in the control of chromatin remodeling and the recruitment of cofactors during significant transcriptional events. It is valuable to note that the approach employed in this study can provide information on the structure of DNA in solution. In particular, the fluorescence-based measurements enable direct measurements of the distance in solution, not limited by crystallizing or electrophoresis conditions. Furthermore, the results presented in this paper are especially important, since the X-ray structure of the natural *hsp27pal* element complexed with the UspDBD and the EcRDBD proteins has not yet been solved.

ACKNOWLEDGMENT

The technical assistance of Mrs. Mirosława Ostrowska is gratefully acknowledged. In addition, we thank Professor Olaf Pongs and Dr. Dirk Isbrandt (Center for Molecular Neurobiology, Hamburg, Germany) for their generous support.

REFERENCES

1. Claessens, F., and Gewirth, D. T. (2004) DNA recognition by nuclear receptors, *Essays Biochem. 40*, 59−72.
2. Lane, D., Prentki, P., and Chandler, M. (1992) Use of gel retardation to analyze protein-nucleic acid interactions, *Microbiol. Rev. 56*, 509−528.
3. Potthoff, S. J., Romine, L. E., and Nardulli, A. M. (1996) Effects of wild type and mutant estrogen receptors on DNA flexibility, DNA bending, and transcription activation, *Mol. Endocrinol. 10*, 1095−1106.
4. Shulemovich, K., Dimaculangan, D. D., Katz, D., and Lazar, M. A. (1995) DNA bending by thyroid hormone receptor: influence of half-site spacing and RXR, *Nucleic Acids Res. 23*, 811−818.
5. Petz, L. N., Nardulli, A. M., Kim, J., Horwitz, K. B., Freedman, L. P., and Shapiro, D. J. (1997) DNA bending is induced by binding of the glucocorticoid receptor DNA binding domain and progesterone receptors to their response element, *J. Steroid Biochem. Mol. Biol. 60*, 31−41.
6. Prendergast, P., Pan, Z., and Edwards, D. P. (1996) Progesterone receptor-induced bending of its target DNA: distinct effects of the A and B receptor forms, *Mol. Endocrinol. 10*, 393−407.
7. Aguinaldo, A. M., Turbeville, J. M., Linford, L. S., Rivera, M. C., Garey, J. R., Raff, R. A., and Lake, J. A. (1997) Evidence for a clade of nematodes, arthropods and other moulting animals, *Nature 387*, 489−493.
8. Yao, T. P., Segraves, W. A., Oro, A. E., McKeown, M., and Evans, R. M. (1992) *Drosophila* ultraspiracle modulates ecdysone receptor function *via* heterodimer formation, *Cell 71*, 63−72.
9. Thomas, H. E., Stunnenberg, H. G., and Stewart, A. F. (1993) Heterodimerization of the *Drosophila* ecdysone receptor with retinoid X receptor and ultraspiracle, *Nature 362*, 471−475.
10. Andres, A. J., Fletcher, J. C., Karim, F. D., and Thummel, C. S. (1993) Molecular analysis of the initiation of insect metamorphosis: a comparative study of *Drosophila* ecdysteroid-regulated transcription, *Dev. Biol. 160*, 388−404.
11. Hu, X., Cherbas, L., and Cherbas, P. (2003) Transcription activation by the ecdysone receptor (EcR/USP): identification of activation functions, *Mol. Endocrinol. 17*, 716−731.
12. Niedziela-Majka, A., Kochman, M., and Ożyhar, A. (2000) Polarity of the ecdysone receptor complex interaction with the palindromic response element from the *hsp27* gene promoter, *Eur. J. Biochem. 267*, 507−519.
13. Khorasanizadeh, S., and Rastinejad, F. (2001) Nuclear-receptor interactions on DNA-response elements, *Trends Biochem. Sci. 26*, 384−390.
14. Riddihough, G., and Pelham, H. R. B. (1987) An ecdysone response element in the *Drosophila hsp27* promoter, *EMBO J. 6*, 3729−3734.
15. Ożyhar, A., Strangmann-Diekmann, M., Kiltz, H. H., and Pongs, O. (1991) Characterization of a specific ecdysteroid receptor-DNA complex reveals common properties for invertebrate and vertebrate hormone-receptor/DNA interactions, *Eur. J. Biochem. 200*, 329−335.
16. Ozers, M. S., Hill, J. J., Ervin, K., Wood, J. R., Nardulli, A. M., Royer, C. A., and Gorski, J. (1997) Equilibrium binding of estrogen receptor with DNA using fluorescence anisotropy, *J. Biol. Chem. 272*, 30405−30411.
17. Wang, X., Graveland-Bikker, J. F., de Kruif, C. G., and Robillard, G. T. (2004) Oligomerization of hydrophobin SC3 in solution: from soluble state to self-assembly, *Protein Sci. 13*, 810−821.
18. Grad, I., Niedziela-Majka, A., Kochman, M., and Ożyhar, A. (2001) Analysis of Usp DNA binding domain targeting reveals critical determinants of the ecdysone receptor complex interaction with the response element, *Eur. J. Biochem. 268*, 3751−3758.
19. Niedziela-Majka, A., Rymarczyk, G., Kochman, M., and Ożyhar, A. (1998) Pure, bacterially expressed DNA-binding domains of the functional ecdysteroid receptor capable of interacting synergistically with the *hsp27* 20-hydroxyecdysone response element. GST-Induced dimerization of DNA-binding domains alters characteristics of their interaction with DNA, *Protein Expression Purif. 14*, 208−220.
20. Kim, J., Zwieb, C., Wu, C., and Adhya, S. (1989) Bending of DNA by gene-regulatory proteins: construction and use of a DNA bending vector, *Gene 85*, 15−23.
21. Förster, T. (1948) Intermolecular energy migration and fluorescence, *Ann. Phys. (Lepzig) 2*, 55−75.
22. Fairclough, R. H., and Cantor, C. R. (1977) in *Methods in Enzymology* (Hirs, C. H. W., and Timasheff, S. N., Eds.) pp 347−379, Academic Press, New York.
23. Clegg, R. M., Murchie, A. I., Zechel, A., and Lilley, D. M. (1993) Observing the helical geometry of double-stranded DNA in solution by fluorescence resonance energy transfer, *Proc. Natl. Acad. Sci. U.S.A. 90*, 2994−2998.
24. Gohlke, C., Murchie, A. I., Lilley, D. M., and Clegg, R. M. (1994) Kinking of DNA and RNA helices by bulged nucleotides observed by fluorescence resonance energy transfer, *Proc. Natl. Acad. Sci. U.S.A. 91*, 11660−11664.
25. Vamosi, G., Gohlke, C., and Clegg, R. M. (1996) Fluorescence characteristics of 5-carboxytetramethylrhodamine linked covalently to the 5′ end of oligonucleotides: multiple conformers of single-stranded and double-stranded dye-DNA complexes, *Biophys. J. 71*, 972−994.
26. Lorenz, M., Hillisch, A., Goodman, S. D., and Diekmann, S. (1999) Global structure similarities of intact and nicked DNA complexed

with IHF measured in solution by fluorescence resonance energy transfer, *Nucleic Acids Res. 27*, 4619−4625.
27. Lakowicz, J. R. (1999) *Priciples of Fluorescence Spectroscopy*, Kluwer Academic Plenum Publishers, New York.
28. Wu, J., Parkhurst, K. M., Powell, R. M., Brenowitz, M., and Parkhurst, L. J. (2001) DNA bends in TATA-binding protein-TATA complexes in solution are DNA sequence-dependent, *J. Biol. Chem. 276*, 14614−14622.
29. Grad, I., Kochman, M., and Ożyhar, A. (2002) Functionality versus strength—Has functional selection taken place in the case of the ecdysteroid receptor response element?, *Acta Biochim. Pol. 49*, 747−756.
30. Ferrari, S., Harley, V. R., Pontiggia, A., Goodfellow, P. N., Lovell-Badge, R., and Bianchi, M. E. (1992) SRY, like HMG1, recognizes sharp angles in DNA, *EMBO J. 11*, 4497−4506.
31. Mischati, C., Feriotto, G., Bianchi, N., and Gambari, R. (1995) A non-radioactive automated protocol to study protein-DNA interactions by DNase I footprinting, *Int. J. Oncol. 6*, 153−156.
32. Melcher, S. E., Wilson, T. J., and Lilley, D. M. (2003) The dynamic nature of the four-way junction of the hepatitis C virus IRES, *RNA 9*, 809−820.
33. Wu, H. M., and Crothers, D. M. (1984) The locus of sequence-directed and protein-induced DNA bending, *Nature 308*, 509−513.
34. Ożyhar, A., and Pongs, O. (1993) Mutational analysis of the interaction between ecdysteroid receptor and its response element, *J. Steroid Biochem. Mol. Biol. 46*, 135−145.
35. Devarakonda, S., Harp, J. M., Kim, Y., Ożyhar, A., and Rastinejad, F. (2003) Structure of the heterodimeric ecdysone receptor DNA-binding complex, *EMBO J. 22*, 5827−5840.
36. Lu, X. J., and Olson, W. K. (2003) 3DNA: a software package for the analysis, rebuilding and visualization of three-dimensional nucleic acid structures, *Nucleic Acids Res. 31*, 5108−5121.
37. Strahs, D., and Schlick, T. (2000) A-Tract bending: insights into experimental structures by computational models, *J. Mol. Biol. 301*, 643−663.
38. Dragan, A. I., Liu, Y., Makeyeva, E. N., and Privalov, P. L. (2004) DNA-binding domain of GCN4 induces bending of both the ATF/CREB and AP-1 binding sites of DNA, *Nucleic Acids Res. 32*, 5192−5197.
39. Wright, P. E., and Dyson, H. J. (1999) Intrinsically unstructured proteins: re-assessing the protein structure−function paradigm, *J. Mol. Biol. 293*, 321−331.
40. Tompa, P. (2003) Intrinsically unstructured proteins evolve by repeat expansion, *BioEssays 25*, 847−855.
41. Tompa, P. (2005) The interplay between structure and function in intrinsically unstructured proteins, *FEBS Lett. 579*, 3346−3354.
42. Orłowski, M., Szyszka, M., Kowalska, A., Grad, I., Zoglowek, A., Rymarczyk, G., Dobryszycki, P., Krowarsch, D., Rastinejad, F., Kochman, M., and Ożyhar, A. (2004) Plasticity of the ecdysone receptor DNA binding domain, *Mol. Endocrinol. 18*, 2166−2184.
43. Vlahovicek, K., Kajan, L., and Pongor, S. (2003) DNA analysis servers: plot.it, bend.it, model.it and IS, *Nucleic Acids Res. 31*, 3686−3687.

BI051354B